

RESEARCH

Open Access



Improve the cytotoxic effects of megavoltage radiation treatment by Fe₃O₄@Cus–PEG nanoparticles as a novel radiosensitizer in colorectal cancer cells

Mahshid Mohammadian¹, Soraya Emamgholizadeh Minaei^{2*}  and Amin Shiralizadeh Dezfuli³

*Correspondence:
minayee.s@gmail.com;
emamgholizadeh.s@umsu.ac.ir

¹ Department of Medical Laboratory Sciences, Urmia University of Medical Sciences, Urmia, Iran

² Department of Medical Physics and Imaging, School of Allied Medical Sciences, Urmia University of Medical Sciences, P. O. Box: 5756115198, Urmia, Iran

³ Ronash Technology Pars Company, Tehran, Iran

Abstract

Background: To enhance the performance of radiotherapy, emerging nanoparticles that can professionally enhance X-ray irradiation to destruct cancer cells are extremely necessary. Here, we examined the potential of PEG-coated magnetite copper sulfide hetero-nanoparticles (Fe₃O₄@Cus–PEG) as a radiosensitizer agent.

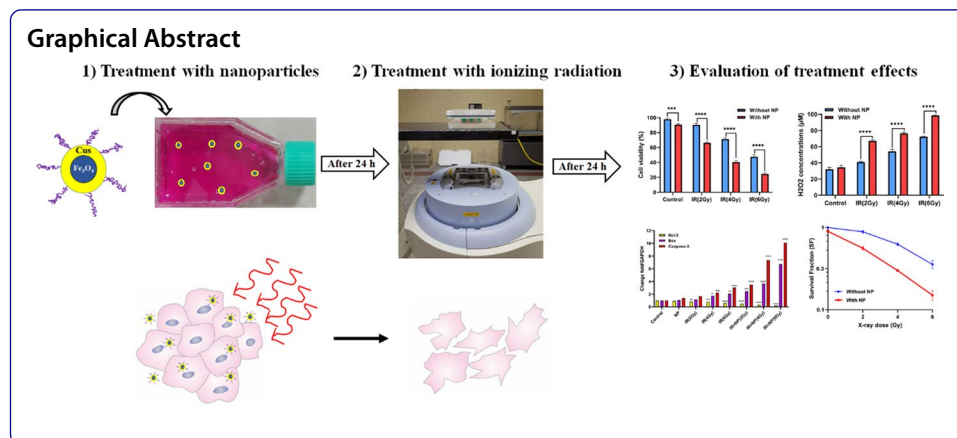
Methods: Fe₃O₄@Cus–PEG nanoparticles were synthesized and characterized. The toxicity of nanoparticles on HT-29 colorectal cancer cells was assessed by the MTT assay. The radio-sensitizing effects of Fe₃O₄@Cus–PEG nanoparticles on HT-29 cancer cells were investigated by the MTT and colony formation assays. Moreover, the underlying mechanisms for Fe₃O₄@Cus–PEG nanoparticles to improve the radiation sensitivity of cells were evaluated.

Results: The results demonstrated that nanoparticles enhanced the effects of X-ray irradiation in a dose-dependent manner. The effects of combined treatments (nanoparticles and X-ray radiation) were strongly synergistic. The sensitizing enhancement ratio (SER) of nanoparticles was 2.02. Our in vitro assays demonstrated that the nitric oxide production, the intracellular hydrogen peroxide concentration, and the expression level of Bax and Caspase-3 genes significantly increased in the cells treated with the combination of nanoparticles and radiation. Whereas, the Glutathione peroxidase enzyme activity and the expression level of the Bcl-2 gene in the combined treatment significantly decreased compared to the radiation alone.

Conclusions: Our study suggests that Fe₃O₄@Cus–PEG nanoparticles are the promising nano radio-sensitizing agents for the treatment of cancer cells to enhance the efficacy of radiation therapy through increasing the reactive oxygen species generation, nitric oxide production, and inducing apoptosis.

Keywords: Colorectal cancer, Radiosensitizer, Ionizing radiation, Copper, Magnetite nanoparticles





Background

Colorectal cancer (CRC) is the third most prevalent cancer worldwide and the second most common cause of cancer death in the United States. It is well-known that surgery, radiotherapy, and chemotherapy are standard treatments for CRC. Meanwhile, the patients' 5-year survival rate is about 65% and for patients with metastatic lesions drops to 12% (Brown et al. 2019; Siegel et al. 2019).

Conventional cancer treatment modalities are associated with their inherent shortcomings. Limitations associated with chemotherapy include systemic toxicity, low tumor-specific selectivity, short half-life in plasma, and development of multidrug resistance (Minaei et al. 2016; Xie et al. 2020). Moreover, one of the greatest challenges in radiation therapy (RT) is the side effects of high doses due to considerations of adjacent healthy tissue radiation tolerance. In addition, radio-resistance of cancer cells is a major issue in radiation therapy and restricts the therapeutic efficacy of radiation (Schaue et al. 2015; Torres-Roca et al. 2008).

Consequently, it would be significantly important to develop new approaches to enhance the treatment efficacy. One of the most effective methods is the combination of radiation therapy with radiosensitizer agents (Huynh et al. 2021; Russell et al. 2021).

In recent years, the application of nanoparticles as radiosensitizers has become a field that has attracted a great deal of attention. The small size of nanoparticles provides a selective accumulation within cancer cells due to the enhanced permeability and retention (EPR) effect that is a tumor characteristic. This selective bio-distribution of nanoparticles limits the surrounding normal tissue side effects and enhances the cancer treatment outcome (Mao et al. 2016; Park et al. 2019).

In the meanwhile, many different types of metal nanoparticles have been reported as radiosensitizers, such as gold (Huynh et al. 2021; Penninckx et al. 2020), hafnium oxide (Chen et al. 2016; Maggiorella et al. 2012), copper (Jiang et al. 2018; Liu et al. 2017), bismuth (Guo et al. 2017; Wang et al. 2016), gadolinium (Delorme et al. 2017; Mi et al. 2015), and iron oxide-based nanoparticles (Nosrati et al. 2021; Russell et al. 2021).

Gold nanoparticles have attracted much attention for dose-enhancing effects because of their good biocompatibility (Goswami et al. 2017; Song et al. 2016). However, it is expensive and more doses of gold nanoparticles are required to achieve significant dose enhancement. To overcome this limitation, we focused on copper and iron oxide nanoparticles for these reasons: they are much cheaper than gold nanoparticles (Huang et al.

2020), can be used in photothermal therapy, and serve as radiosensitizer agents (Hadi et al. 2020; Huang et al. 2019; Russell et al. 2021; Rybka 2019).

Copper (in a suitable dose) is an essential trace mineral for survival and it is present in the structure of human vital enzymes. It is found mostly in the liver, brain, heart, kidneys, and skeletal muscles. Copper (Cu) has a basic role in the immune system, energy production, and maintaining nerve cells. Cu also helps to absorb iron in the body and works with iron to aid the body make red blood cells (Rosanoff et al. 2012; Wang et al. 2019). A suitable dose of copper has the above benefits, but excessive consumption of copper is associated with morphological and metabolic changes in tissues. Excessive accumulation of copper in the tissue can cause various types of diseases (Gupta et al., 2009).

In radiation therapy, megavoltage ionizing radiation mainly interacts with cells through Compton scattering, which produces secondary electrons (physical step) (Binjola 2020). Megavoltage ionizing radiation and secondary electrons induce the radiolysis of water or other molecules around DNA which generates ROS (chemical step). The produced ROS lead to the induction of oxidative stress (Schieber et al. 2014), DNA single and double-strand breaks, and ultimately cause cell death (biological step) (Desouky et al. 2015; LaVerne 2000). Therefore, ionizing radiation interacts with DNA and damages cells directly or indirectly (through ROS).

Therefore, radiation sensitizing nanoparticles capable of generating reactive oxygen species in the presence of radiation exposure may increase lethal effects caused by radiation and enhance the therapeutic efficiency of RT (Babaei et al. 2014).

Recently, it has been shown that copper nanoparticles can enhance ROS production after exposure to ionizing radiation and induce autophagy in cancer cells. To overcome the radioresistance of cancer cells, the induction of autophagy and generation of ROS may be an effective method (Jiang et al. 2019; Liu et al. 2017).

In addition, superparamagnetic iron oxide nanoparticles (SPIONs) have a wide variety of properties and applications that make them suitable for use in nano-medicine. They can be used in magnetic hyperthermia for the treatment of cancer cells, in T2-weighted magnetic resonance imaging (MRI) as a contrast agent, in targeted drug delivery, in image-guided radiotherapy (IGRT), and in the presence of ionizing radiation as a radio enhancer agent through catalyzing the production of ROS in cancer cells (Klein et al. 2012; Sun et al. 2016).

Uncoated nanoparticles are more toxic and have a shorter systemic circulation time due to reticuloendothelial phagocytosis and renal clearance. Therefore, the modification and coating of the surface of nanoparticles with polymers are critical. Many different polymers for, example, poly vinyl pyrrolidone (PVP) (Gupta et al. 2005), poly lactic glycolic acid (PLGA) (Kiamohammadi et al. 2021; Shirvalilou et al. 2020), poly butyl cyanoacrylate (PBCA) (Ghaferi et al. 2020), and polyethylene glycol (PEG) (Gao et al. 2020) have been reported as biocompatible coatings for nanoparticles. In general, PEG is an FDA-approved biodegradable hydrophilic polymer that can enhance the structural and chemical stability of NPs and reduce their cytotoxicity.

Hetero-nanostructures are exhibited stronger radio enhancing effect because of the synergetic interactions of ionizing radiation with an individual component in hetero-nanoparticles (Huang et al. 2019; Zhang et al. 2018). Therefore, in the present study, we

focused on the potential of PEG-coated magnetite copper sulfide hetero-nanoparticles ($\text{Fe}_3\text{O}_4@\text{Cus-PEG}$) to serve as a radiosensitizer agent to enhance the efficacy of radiation therapy. To investigate the corresponding mechanisms for $\text{Fe}_3\text{O}_4@\text{Cus-PEG}$ nanoparticles to improve the radiation sensitivity of cells, colorectal HT-29 cancer cell lines were used and subjected to ionizing radiation in the presence or absence of $\text{Fe}_3\text{O}_4@\text{Cus-PEG}$ NPs. We then evaluated the cytotoxic effects of different treatments based on the ROS production level, the nitric oxide concentration, the glutathione peroxidase enzyme activity, the expression level of apoptosis-related genes, and the cellular metabolic activity. Moreover, the long-term cytotoxicity of treatments was investigated by the colony formation assay.

Materials and methods

Materials

Carboxylated polyethylene glycol was purchased from AMINBIC. Ethylene glycol, $\text{FeCl}_3 \cdot 6\text{H}_2\text{O}$, $\text{FeCl}_2 \cdot 4\text{H}_2\text{O}$, Sodium thiosulfate pentahydrate ($\text{Na}_2\text{S}_2\text{O}_3 \cdot 5\text{H}_2\text{O}$), and copper sulfate (CuSO_4) were obtained from Merck Company (Darmstadt, Germany). Dimethyl sulfoxide (DMSO) and 3-(4,5-Dimethyl-thiazol-2-yl)-2,5-diphenyl-tetrazolium bromide (MTT) were purchased from Sigma Company (St. Louis, MO, USA). Penicillin-streptomycin, fetal bovine serum (FBS), Roswell Park Memorial Institute (RPMI) 1640, and Trypsin-EDTA (0.25%) were provided from Gibco (Invitrogen, USA). The nitric oxide assay kit was obtained from Biocore Diagnostik Company (ZellBio GmbH, Germany). The fluorimetric hydrogen peroxide assay kit was prepared from Sigma-Aldrich Company (St. Louis, MO, USA). cDNA synthesis kit and SYBR Green qPCR Master Mix were purchased from Takara company (Takara Bio Inc., Japan). Furthermore, HT-29 cell lines were obtained from the Pasteur Institute of Iran.

Synthesis of nanoparticles

For preparation of SPIONs (Fe_3O_4), a solution of FeCl_3 and FeCl_2 was prepared in a molar ratio of 2:1 ($\text{FeCl}_3 = 3.2442$ g and $\text{FeCl}_2 = 1.2675$ g in 25 mL deionized water) and stirred under an N_2 atmosphere at 90 °C. In the next step, an adequate amount of 28% ammonia was added to the solution to the pH of 10. After 30 min stirring, the resultant product was washed three times with deionized water to remove impurities and then dried.

0.15 g of magnetite nanoparticles were dispersed in 20 mL of pure ethylene glycol and stirred at 120 °C. Thereafter, 0.8 g of CuSO_4 and 1.9 g of $\text{Na}_2\text{S}_2\text{O}_3 \cdot 5\text{H}_2\text{O}$ were added to the solution, respectively, and refluxed for 90 min at 140 °C. Finally, the formed product was washed three times with deionized water and then dried.

Carboxylated polyethylene glycol was used to functionalize the surface of nanoparticles. For this purpose, 0.1 g of nanoparticles obtained from the previous step were dispersed in 20 mL of deionized water by ultrasound for 60 min. Subsequently, 10 mL of a solution containing 50 mg of polyethylene glycol carboxyl was added to it and sonicated for 20 min. Thereafter, the solution was stirred at room temperature for 24 h. Finally, the resultant product was washed three times with deionized water and dried. The obtained nanoparticles were stored in dried form.

Characterization of nanoparticles

The morphology of Fe₃O₄ and Fe₃O₄@Cus-PEG NPs were characterized by transmission electron microscope (TEM) (Zeiss LEO906, Jena, Germany) at 100 kV. The mean hydrodynamic diameter and size distribution of synthesized nanoparticles were determined using a dynamic light scattering (DLS) system (Nanoflex, Particle Metrix, Germany).

The X-ray diffraction (XRD) spectra of Fe₃O₄@Cus NPs were determined using an D8-advance (Bruker, Germany) powder diffractometer equipped with a Cu K α radiation source ($\lambda = 1.54187 \text{ \AA}$) and scanned in a range from 20 to 80°.

Biological experiments

Cell culture

The experiments were performed on human colorectal adenocarcinoma (HT-29) cell line. The cell lines were cultured in RPMI-1640 culture medium, supplemented with 10% fetal bovine serum (FBS) and 1% penicillin–streptomycin, and incubated at 37 °C in 5% CO₂. The experiments were carried out in the logarithmic phase of cell growth.

Analysis of cytotoxicity

3-(4, 5dimethylthiazol-2-yl)-2, 5-diphenyltetrazolium bromide (MTT) assay was used to assess the cytotoxicity of Fe₃O₄@Cus-PEG NPs on the HT-29 cell lines. The cells at a density of 8×10^3 cells/well were seeded in a 96 well-plate and incubated in RPMI-1640 medium at 37 °C in 5% CO₂ for 24 h. Then, the culture medium was replaced with one containing different concentrations of Fe₃O₄@Cus-PEG NPs (0, 0.5, 5, 10, 20, 25, 30, and 40 mg/mL) and incubated for an additional 24 h. After that, the medium was discarded and 100 μ L of MTT solution (5 mg of MTT powder was dissolved in 1 mL of PBS) was added to each well and incubated for 4 h. The viable cells can reduce the tetrazolium salt to formazan crystals, which have a purple color. After incubation for 4 h, the MTT solution was removed and the formazan crystals were dissolved with 100 μ L DMSO. The relative viability was determined by measuring the optical density (OD) of samples at 570 nm. This experiment was carried out in triplicate and repeated three times. The percentage of cell viability was calculated according to Eq. 1 and plotted as a function of nanoparticle concentrations:

$$\text{Cell viability(\%)} = \frac{\text{average OD of treated samples}}{\text{average OD of untreated samples}} \times 100 \quad (1)$$

Moreover, the inhibitory concentration values (IC₅₀ and IC₁₀) of nanoparticles were calculated based on the dose–response curve using the Compusyn software.

Radiation treatment and radio-sensitivity evaluation of cancer cells

To evaluating the in vitro radio-sensitization effects of the synthesized nanoparticles, HT-29 cell lines were treated in eight groups: (1) control, (2) Fe₃O₄@Cus-PEG NPs (5 mg/mL), (3) 2 Gy X-rays, (4) 4 Gy X-rays, (5) 6 Gy X-rays (6) NPs + 2 Gy X-rays, (7) NPs + 4 Gy X-rays, and (8) NPs + 6 Gy X-rays.

After culturing HT-29 cell lines for 24 h (at a density of 10^4 cells/cm²), the cells were treated with Fe₃O₄@Cus-PEG nanoparticles at the concentration of 5 mg/mL. After

24 h treatment, HT-26 cells were washed three times to remove traces of NPs. Subsequently, the cells were irradiated with 6-MV X-ray photons (200 cGy/min) from a medical linear accelerator (Siemens, Germany) at doses of 0, 2, 4, and 6 Gy X-rays and incubated for an additional 24 h.

To evaluate the cytotoxicity effects of various treatments and radio-sensitization effects of NPs, MTT assay, reactive oxygen species analysis, Nitric oxide (NO) assay, glutathione peroxidase (GPX) enzyme activity measurement, colony formation analysis, and quantitative real-time PCR (q-RT-PCR) assay for Bax, Bcl-2, and caspase-3 genes were performed.

Metabolic assay The effects of various treatments on metabolic activity and cell viability were assessed by MTT assay. After treating the cells with ionizing radiation or nanoparticles, the cells were incubated for 24 h. Afterward, the culture medium was replaced with MTT solution and the assay was performed as described in section "[Analysis of cytotoxicity](#)". The activity of NADH-dependent cellular oxidoreductase enzymes reveals the number of viable cells present.

The long-term cytotoxicity of treatments Cell survival and long-term cytotoxicity of treatments were quantified using the clonogenic assay. After treatment as described in section "[Radiation treatment and radio-sensitivity evaluation of cancer cells](#)", the HT-29 cells were re-cultured in 60 mm Petri dishes and incubated in the presence of RPMI-1640 culture medium supplemented with 10% FBS for 8 days at 37 °C and 5% CO₂ humidified atmosphere.

The number of seeded cells per dish should be appropriate with the type of treatment to obtain the countable number of colonies. Therefore, the number of cultured cells for control, Fe₃O₄@Cus-PEG NPs, 2 Gy X-rays, 4 Gy X-rays, 6 Gy X-rays, NPs + 2 Gy X-rays, NPs + 4 Gy X-rays, and NPs + 6 Gy X-ray groups were 200, 200, 500, 1000, 2000, 1000, 2000, and 4000, respectively.

After 8 days, the cells were fixed with a 2% formaldehyde solution for 15 min and stained with Crystal Violet for 20 min. The photographic images of Petri dishes containing colonies were prepared and the number of cell colonies (a group of more than 50 cells) was counted. The plating efficiency (PE) was calculated according to Eq. 2. This was used to determine the surviving fraction (SF) for each treatment by Eq. 3:

$$PE (\%) = \frac{\text{The number of colonies counted}}{\text{The number of cell seeded}} \times 100 \tag{2}$$

$$SF = \frac{PE \text{ treated}}{PE \text{ control}} \tag{3}$$

Moreover, survival curves were plotted as survival fractions against radiation doses (alone or combined with NPs) and fitted to the Linear Quadratic Model by OriginPro software according to the following equation:

$$SF = \exp^{-\alpha D - \beta D^2} \tag{4}$$

where SF is the cell survival fraction, D is the radiation dose (Gy), α is a single hit that induces double-strand break (DSB) of two chromosomes (linear part of the curve), and β is double hits that induce DSB of two chromosomes (quadratic part of the curve). The parameters of α , β , D_{10} , D_{37} , D_{50} , and SF_2 were obtained from the curves. D_{10} , D_{37} , and D_{50} are doses necessary to reduce the SF of cells to 10%, 37%, and 50%, respectively. SF_2 is the survival fraction of cells at 2 Gy X-rays. The sensitivity enhancement ratio (SER) is a principal factor to determine the efficacy of radiosensitizer agents. The SER of $Fe_3O_4@Cus-PEG$ nanoparticles was calculated using the following equation:

$$SER = \frac{D_{50}(\text{without sensitizer})}{D_{50}(\text{with sensitizer})} \quad (5)$$

Cellular ROS measurement To determine the amount of intracellular hydrogen peroxides as reactive oxygen species that were generated by X-ray radiation or nanoparticles, the Fluorescent Hydrogen Peroxide assay Kit (Sigma-Aldrich Company) was used. Master mix solution was prepared according to the kit manual. After 24 h of cell treatments, 50 μ L of the Master mix solution was added into each sample and the cells were incubated for 30 min at room temperature. Peroxidase substrate generates a red fluorescent product after reacting with the intracellular hydrogen peroxides. The fluorescence intensity was measured by a fluorescent microplate reader at 540 nm excitation and 590 nm emission. The concentration of intracellular hydrogen peroxides produced by various treatments is proportional to the fluorescence intensity.

Nitric oxide (NO) assay Nitric oxide has a very short half-life, but its content can be calculated indirectly by measuring concentrations of nitrates and nitrites in biological fluids by the nitric oxide assay. According to the kit manual (ZellBio GmbH, Germany), the supernatants of samples were carefully collected and 300 μ L of the samples were added to the related name test tubes. 10 μ L R1 reagent was added to each tube and the tubes were centrifuged. Subsequently, 100 μ L supernatants of the tubes and 100 μ L standards were transferred into related microwells. 100 μ L ready R2, 50 μ L ready R3, and 50 μ L ready R4 were added into all wells and incubated for 30 min at 37 °C. Nitrates and nitrites in the solutions can react with the chromogenic agent and produce a pink compound. The color intensity was measured by the microplate reader at 540 nm and is proportional to the nitric oxide concentration.

Glutathione peroxidase (GPX) enzyme activity measurement Glutathione Peroxidase is an anti-oxidant enzyme and catalyzes the reduction of hydrogen peroxide to water by reducing glutathione. GPX has a key role to protect the cells from oxidative damage. After 24 h of cell treatments, the supernatants of samples were collected and the GPX enzyme activity was quantified using the ZellBio GmbH assay kit according to the manual (ZellBio GmbH, Germany). Finally, the yellow color intensity was measured by the microplate reader at 412 nm and indirectly related to the GPX enzyme activity.

Quantitative real-time polymerase chain reaction (qRT-PCR) analysis To investigate apoptosis as one of the mechanisms involved in the death of cancer cells, the expres-

sion of apoptotic-related genes (Bax, Bcl-2, and caspase-3) was evaluated by q-RT-PCR analysis. Following the treatments, RNA was extracted from cells using a Trisol solution (Gene all, South Korea) according to the kit manual. Total RNA was reverse transcribed into the single-strand complementary DNA (cDNA) using the Prime Script cDNA synthesis kit (Takara Bio Inc., Japan). The primer sequences were as follows:

Bcl-2.

F 5'-CTGTGGATGACTGAGTACCTG-3'

R 5'-GAGACAGCCAGGAGAAATCA-3'

Bax

F 5'-GACTCCCCCGAGAGGTCTT-3'

R 5'-ACAGGGCCTTGAGCACCAGTT-3'

Caspase-3

F 5'-TGTCATCTCGCTCTGGTACG-3'

R 5'-AAATGACCCCTTCATCACCA-3'

Housekeeping gene (GAPDH)

F 5'-CAAGATCATCAGCAATGCCT-3'

R 5'-GCCATCAGCCACAGTTTCC-3'.

Real-time PCR was performed on an ABI Plus one system using SYBR[®] Premix Ex Taq[™] (Takara Bio Inc., Japan). The reaction conditions were pre-denaturation at 94 °C for 3 min; followed by 40 cycles of denaturation at 94 °C for 10 s, annealing at 59 °C for 30 s, and extension at 72 °C for 20 s. The expression of Bax, Bcl-2, and Caspase-3 genes was normalized to the housekeeping gene and quantified using the $2^{-\Delta\Delta C_t}$ method.

Combined effect of nanoparticles and ionizing radiation The combined effects of Fe₃O₄@Cus-PEG NPs and ionizing radiation (at different doses) were evaluated using equations established by Ito et al. (Ito et al., 2007). [NP], [IR], and [NP + IR] representative the percentage of cell viability after treatments with Fe₃O₄@Cus-PEG NPs, ionizing radiation, and a combination of nanoparticles with ionizing radiation, respectively. The combined effects were calculated as follows:

[NP + IR] < [NP] × [IR]/100, synergistic effect.

[NP + IR] = [NP] × [IR]/100, additive effect.

[IR] < [NP + IR], if [NP] < [IR], antagonistic effect.

Statistical analysis

All assays were carried out in triplicate and repeated three times. Data were presented as mean ± standard deviation (SD). To statistically analyze the data, one-way analysis of variance (ANOVA) analysis was performed by GraphPad Prism software (version 6). $P < 0.05$ was considered to be statistically significant.

Results

Characterization of nanoparticles

TEM images of Fe₃O₄ and Fe₃O₄@Cus-PEG nanoparticles (Fig. 1A, B) demonstrated that the nanoparticles had semi-spherical morphology. The average size of Fe₃O₄ and Fe₃O₄@Cus-PEG nanoparticles were about 15 and 25 nm, respectively, which were

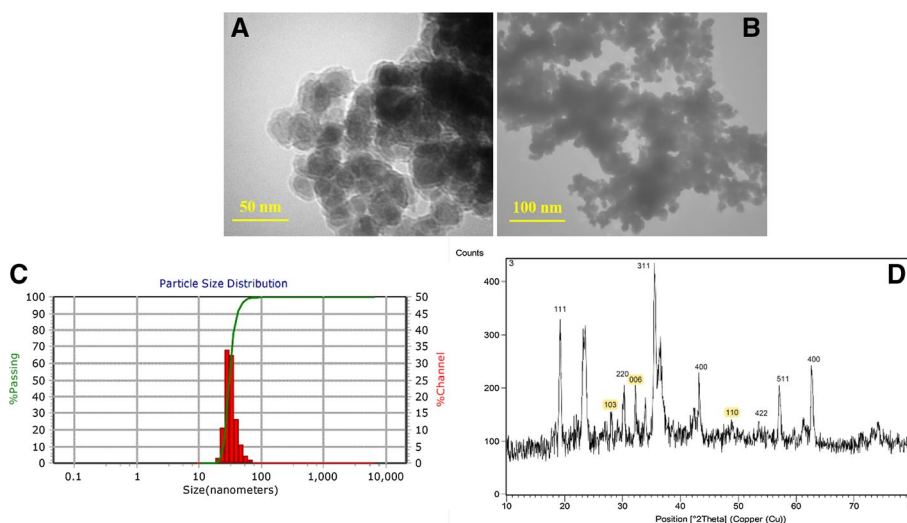


Fig. 1 Characterization of nanoparticles. Transmission electron microscopic images of **A** $\text{Fe}_3\text{O}_4@\text{Cus-PEG}$ and **B** Fe_3O_4 nanoparticles. **C** Dynamic light scattering result of $\text{Fe}_3\text{O}_4@\text{Cus}$ nanoparticles, and **D** X-ray diffraction pattern of $\text{Fe}_3\text{O}_4@\text{Cus}$ nanoparticles

measured using standard software (Image J). As illustrated in Fig. 1C, the mean hydrodynamic diameter of $\text{Fe}_3\text{O}_4@\text{Cus-PEG}$ measured using DLS was 31 nm, which was slightly larger than the size measured by TEM images. This difference can be explained by the absorption of liquid and the formation of a hydration layer around nanoparticles.

Figure 1D shows the XRD pattern of $\text{Fe}_3\text{O}_4@\text{Cus}$ nanoparticles. All the diffraction peaks shown in black at $2\theta = 19.27, 23.62, 30.36, 35.85, 43.63, 53.52, 57.48,$ and 63.2 are related to the hexagonal arrangement of iron nanoparticles (JCPDS card NO. 65-3556). The marked yellow peaks at $2\theta = 28.135, 32.267,$ and 48.674 correspond to the crystal-line plan of Cus. The weak diffraction intensity indicates Cus was amorphously placed on the surface of Fe_3O_4 (Zhang et al. 2017).

Biological experiments

Analysis of cytotoxicity

Before any biological experiments, the MTT assay was used to determine the potential cytotoxicity effect $\text{Fe}_3\text{O}_4@\text{Cus-PEG}$ of NPs on the HT-29 cell line. According to Fig. 2, nanoparticles caused concentration-dependent toxicity in HT-29 cells.

The IC50 and IC10 values for NPs after 24 h treatment were calculated using the CompuSyn software and were equal to 22.26 and 5 mg/mL, respectively. According to the results of MTT assay, 5 mg/mL of $\text{Fe}_3\text{O}_4@\text{Cus-PEG}$ NPs which induced low toxicity (about 10%) was chosen for the subsequent experiments.

Radiation treatment and radio-sensitivity evaluation of cancer cells

As mentioned previously, $\text{Fe}_3\text{O}_4@\text{Cus-PEG}$ NPs are assumed to significantly enhance the effects of ionizing radiation on cancer cells. To reveal the interactions between nanoparticles and ionizing radiation, the in vitro assays were performed on the treated HT-29 colorectal cancer cells.

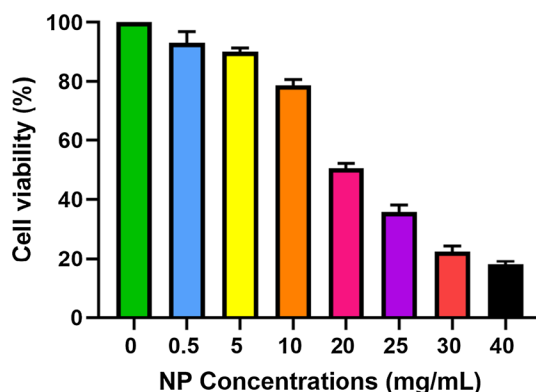


Fig. 2 Viabilities of HT-29 cells after treatment with different concentrations of Fe₃O₄@Cus-PEG nanoparticles for 24 h determined by the MTT assay (mean ± SD, n = 3)

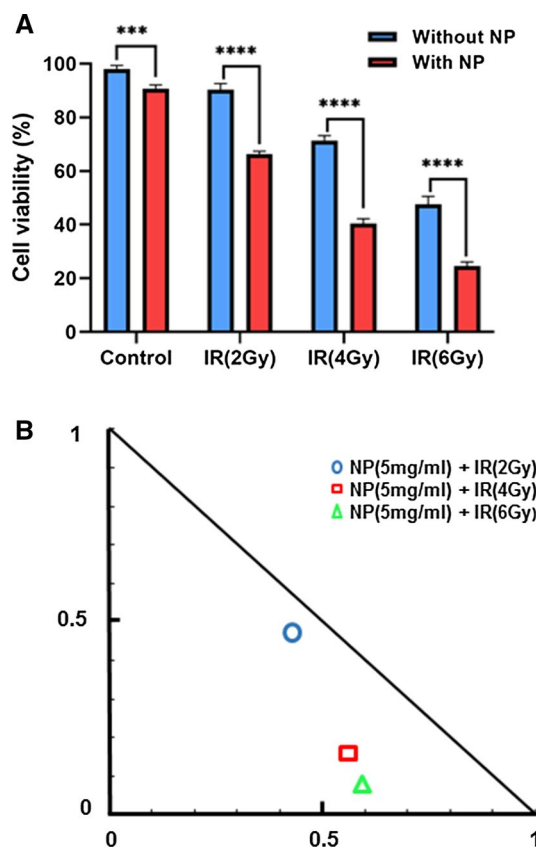


Fig. 3 **A** Viabilities of HT-29 cells exposed to 0, 2, 4, and 6 Gy ionizing radiation (IR) in the presence or absence of Fe₃O₄@Cus-PEG nanoparticles measured by the MTT assay (mean ± SD, n = 3) (***) $P < 0.001$ and **** $P < 0.0001$. **B** Isobologram curve of the synergistic effects of different combined treatments applied to HT-29 cells

Metabolic assay MTT assay was used to examine the radio-sensitizing effects of Fe₃O₄@Cus-PEG NPs under different doses of X-ray radiation. The results in Fig. 3A show that the cell viability decreased in an X-ray dose-dependent way with or without nanoparti-

cles. By increasing the absorbed radiation dose, the amount of energy transferred per unit mass increases. Therefore, the probability of radiation interaction with nanoparticles or cells increases, which can lead to an increase in the ionization rate, DNA damage, and ultimately a decrease in cell viability.

The viability of HT-29 cells treated with 2 Gy ionizing radiation was $90.4\% \pm 1.2$. Whereas, when cancer cells were treated with nanoparticles before exposure to 2 Gy IR, the cell viability was significantly reduced to $62.5\% \pm 2.9$ ($P < 0.0001$). In addition, in the absence of NPs, the cell viability was $71.38\% \pm 2.2$ and $47.5\% \pm 1.8$ under 4 and 6 Gy X-ray radiation, respectively. However, the cell viability under 4 and 6 Gy IR in the presence of NPs significantly decreased to $40.3\% \pm 1.8$ and $24.6\% \pm 1.8$, respectively.

The effectiveness of combination treatments (X-ray radiation and $\text{Fe}_3\text{O}_4@\text{Cus-PEG}$ nanoparticles) was evaluated by the Compusyn software using the combination index (CI). CI < 1, equal to 1, and > 1 represent synergism, additivity, and antagonism, respectively (Rae et al. 2013). The CI values for the combined treatments of $\text{Fe}_3\text{O}_4@\text{Cus-PEG}$ NPs and X-ray radiation at doses of 2, 4, and 6 Gy were equal to 0.88 ± 0.03 , 0.73 ± 0.3 , and 0.67 ± 0.02 , respectively. These results indicated that NPs and ionizing radiation had synergetic effects on the HT-29 cells.

Moreover, for further investigation, the isobologram curve obtained from the Compusyn software was evaluated for the combination treatment of nanoparticles and different doses of X-rays. In the isobologram curve, if points are on the line, the relationship between nanoparticles and ionizing radiation is an additive effect. In addition, if points are below or above the line, the interaction between combination treatments is synergism and antagonism effect, respectively. As shown in Fig. 3B, the effects of NPs and IR at different doses on HT-29 colorectal cancer cells were synergistic, because all points for different combination treatments in the isobologram curve were below the line of an additive effect. As can be seen, the results of the isobologram curve were consistent with the results obtained from the combination index.

The long-term cytotoxicity of treatments To further examine the radio-sensitization effect of $\text{Fe}_3\text{O}_4@\text{Cus-PEG}$ NPs, the clonogenic assay was conducted. As depicted in Fig. 4B, C, the number of colonies and cell surviving fraction decreased with increasing doses of X-ray radiation (in the absence or presence of NPs). Surviving fractions of NPs-pretreated HT-29 cells under X-ray radiation were significantly lower than that of ionizing radiation alone at the same doses ($P < 0.0001$). The SF of NP-treated cells followed by 0, 2, 4, and 6 Gy X-ray radiation were equal to 0.9 ± 0.001 , 0.56 ± 0.04 , 0.32 ± 0.026 , and 0.15 ± 0.2 , respectively (Fig. 4).

Data obtained from survival curves showed that the presence of nanoparticles under X-ray irradiation enhanced the damages of cells.

Table 1 shows the extracted parameters from the survival curves fitted to the LQ model. As illustrated in Table 1, the α parameter increased in the combined group (NP + IR) compared to the ionizing radiation alone group, while the β parameter exhibited a reverse tendency and decreased. Compared to X-ray radiation alone, the values of SF_2 , D_{10} , D_{37} , and D_{50} parameters decreased during X-rays in the presence of NPs.

The sensitizing enhancement ratio (SER) of $\text{Fe}_3\text{O}_4@\text{Cus-PEG}$ nanoparticles was approximately 2.02 which indicates that the presence of nanoparticles doubles the

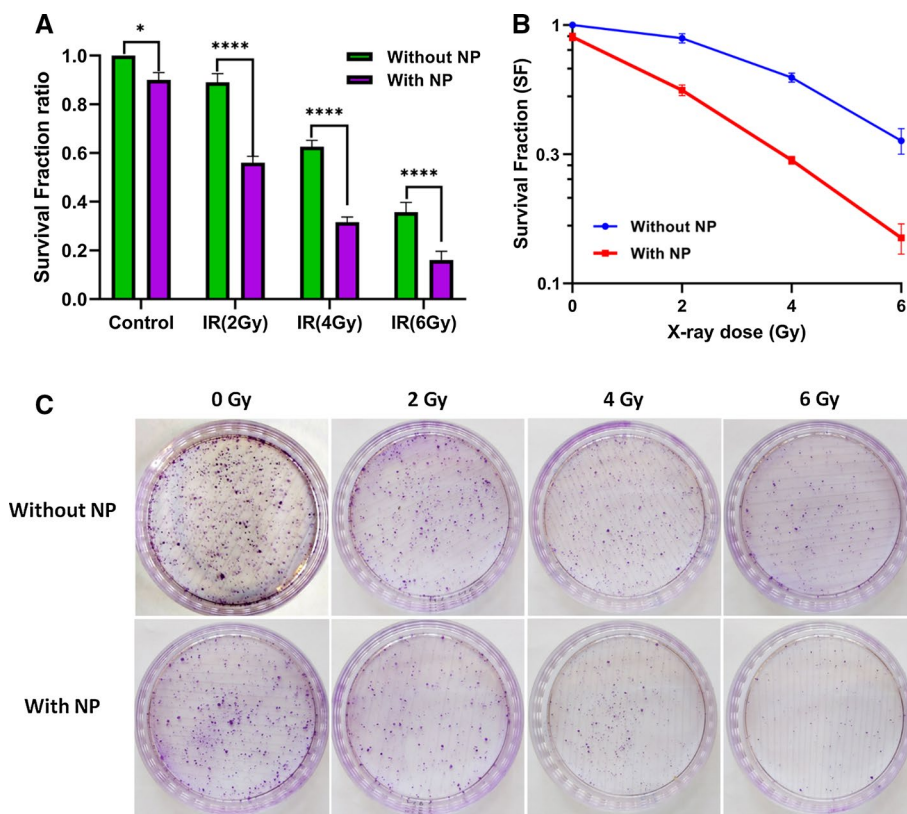


Fig. 4 **A** Survival fraction of HT-29 cancer cells treated with the ionizing radiation (IR) with or without Fe₃O₄@Cus-PEG nanoparticles measured by the clonogenic assay. **B** Cell survival curves as a function of X-ray dose at the presence and absence of nanoparticles. **C** Images of colonies formed by M HT-29 cells after various treatments. Data were represented the mean ± SD of three independent experiments (*****P* < 0.0001)

Table 1 Radiobiological parameters of HT-29 cells survival curves fitted to the LQ model

Groups	α (Gy ⁻¹)	β (Gy ⁻¹)	SF ₂ (Gy)	D ₁₀ (Gy)	D ₃₇ (Gy)	D ₅₀ (Gy)	SER
IR without NPs	0.0025	0.028	0.89	8.99	5.89	4.91	2.02
IR with NPs	0.27	0.006	0.57	7.33	3.42	2.43	

IR: ionizing radiation; NPs: nanoparticles; SER: sensitizing enhancement ratio

damage caused by ionizing radiation. Overall, these results reveal that Fe₃O₄@Cus-PEG NPs have a significant radio-sensitization potential on HT-29 colorectal cancer cells.

Cellular ROS measurement Figure 5A illustrates the concentration of hydrogen peroxides in HT-29 cancer cells treated with Fe₃O₄@Cus-PEG NPs and different doses of X-ray exposure. Obtained results of H₂O₂ generation in the cells treated with 5 mg/mL nanoparticles (in the absence of ionizing radiation), showed no significant ROS production in comparison with the control sample (*P* > 0.05).

HT-29 cells receiving both Fe₃O₄@Cus-PEG NPs and ionizing radiation (at all doses) had a significant increase in the level of H₂O₂ concentration compared to the cells treated with the ionizing radiation alone (*P* < 0.0001). Furthermore, when NPs-treated cells were exposed to X-ray irradiation, the H₂O₂ concentration level

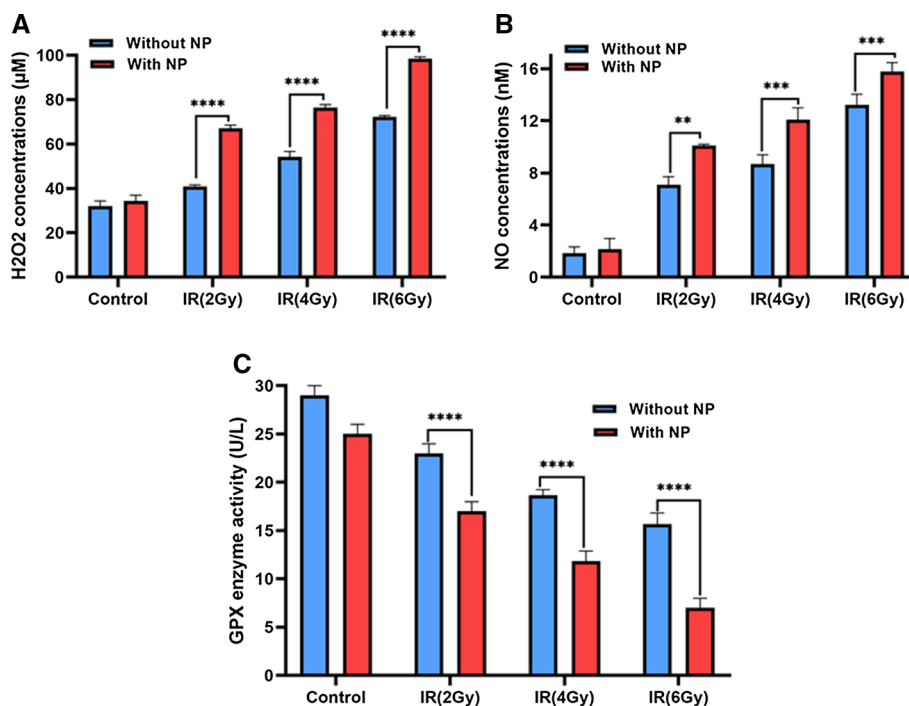


Fig. 5 Effects of ionizing radiation (IR) with or without Fe₃O₄@Cus-PEG nanoparticles on HT-29 colorectal cancer cells in **A** H₂O₂ concentration, **B** nitric oxide (NO) concentration, and **C** glutathione peroxidase (GPX) enzyme activity. Data were represented the mean ± SD of three independent experiments. Statistical significance was showed with **P* < 0.05, ***P* < 0.01, ****P* < 0.001, and *****P* < 0.0001, respectively

increased with increasing the radiation doses. These data demonstrated that Fe₃O₄@Cus-PEG NPs in the presence of X-ray irradiation could significantly increase the intracellular H₂O₂ (as a ROS) generation.

Nitric oxide (NO) assay Nitric oxide is a critical radical responsible for the balance between oxidants and antioxidants of each cell. Intracellular NO level was assessed using the NO colorimetric assay and the results are shown in Fig. 5B. As can be seen, there was no significant difference between the NPs-treated and untreated cells (*P* > 0.05). Relative to untreated cells, the NO level increased by 3.83, 4.68, and 7.14-fold for the cells treated by 2, 4, and 6 Gy ionizing radiation, respectively. In addition, pretreatment of HT-26 cells with Fe₃O₄@Cus-PEG NPs followed by 2, 4, and 6 Gy X-ray radiation showed a 5.45, 6.53, and 8.54-fold increase in NO level compared to the control sample, respectively. In particular, the assay proved that the intracellular NO level was significantly elevated by the combination of Fe₃O₄@Cus-PEG NPs and ionizing radiation.

Glutathione peroxidase (GPX) enzyme activity measurement The results of the Glutathione peroxidase enzyme activity are shown in Fig. 5C. The GPX enzyme activity in HT-29 cells treated with 0, 2, 4, and 6 Gy ionizing radiation was equal to 29 ± 1, 23 ± 1, 18.67 ± 0.5, 15.67 ± 1.1, respectively. Whereas, GPX enzyme activity reduced to 25 ± 1.01, 17 ± 1.15, 11.83 ± 1.04, and 7 ± 0.98, respectively in the cells treated with the combination of Fe₃O₄@Cus-PEG NPs and X-rays (at the same doses).

In our study, H₂O₂ as a main component of oxidative stress mediator were up-regulated in the cells treated with ionizing radiation in the presence of nanoparticles. Excess ROS stress produced in cancer cells can affect the antioxidant capacity of cancer cells and reduce the activity level of antioxidant enzymes (such as glutathione peroxidase enzyme) and thereby disrupt the redox homeostasis in cancer cells (Hauser et al. 2016).

From our results, HT-29 cells treated with nanoparticles and X-rays manifested a remarkable reduction in the level of GPX enzyme activity compared to the group treated with the X-ray radiation alone ($P < 0.0001$).

Quantitative real-time polymerase chain reaction (qRT-PCR) analysis To better understand the mechanisms of X-ray and nanoparticles, the mRNA expression levels of the apoptotic-related genes (Bax, Bcl-2, and caspase-3) were evaluated using the qRT-PCR analysis. As illustrated in Fig. 6A, the mRNA expression level of Bax and caspase-3 genes increased in an X-ray dose-dependent manner, whereas the expression level of Bcl-2 gene decreased. Fe₃O₄@Cus-PEG NPs at the concentration of 5 mg/mL did not change significantly the mRNA expression levels of Bax, caspase-3, and Bcl-2 genes in comparison with

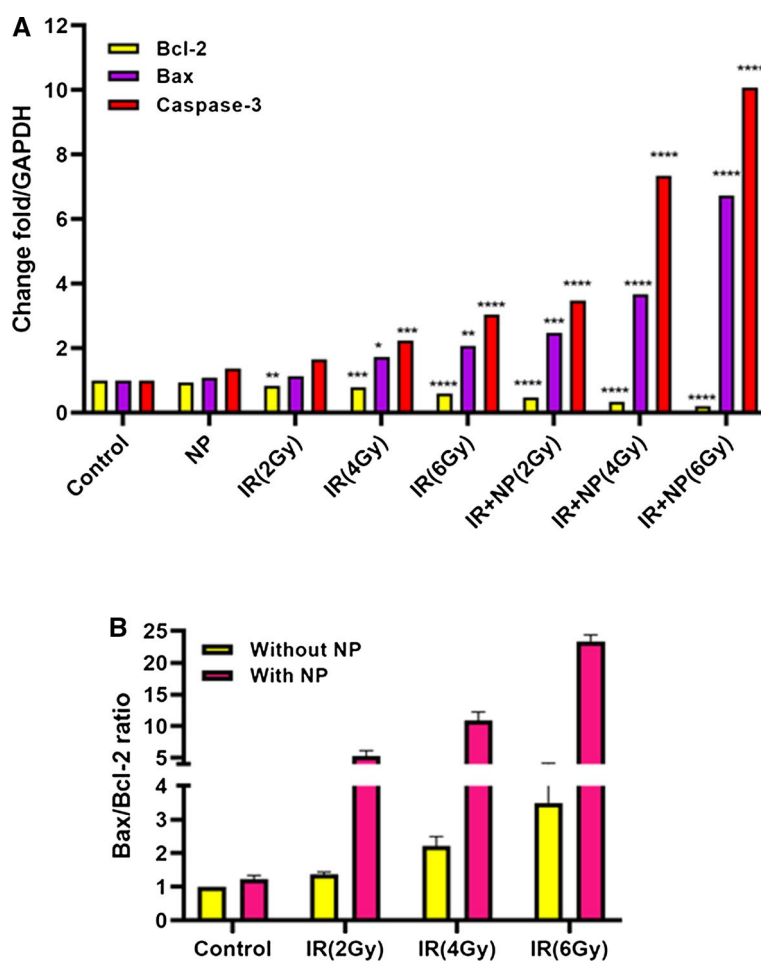


Fig. 6 **A** mRNA expression level of Bax, Bcl-2, and caspase-3 genes and **B** Bax/Bcl-2 mRNA ratio in HT-29 cells after various treatments determined by qRT-PCR technique (mean ± SD, n = 3). * $P < 0.05$, ** $P < 0.01$, *** $P < 0.001$, and **** $P < 0.0001$ significant with respect to the control

the control sample ($P > 0.05$). Figure 6A shows that HT-29 cells treated with Fe₃O₄@Cus-PEG nanoparticles and ionizing radiation (at all doses) had a significant increase in the expression levels of Bax and caspase-3 genes and a notable decrease in the Bcl-2 mRNA expression compared to the cells treated with ionizing radiation alone ($P < 0.0001$). For example, the expression levels of Bax and caspase-3 in the cells treated with NPs + 6 Gy X-ray increased by 2.38 and 3.32-fold compared to the X-ray alone groups, respectively ($P < 0.0001$). Inversely, the combination of 6 Gy X-ray with NPs decreased the Bcl-2 expression level by 2.86-fold.

In the stimulation of the intrinsic pathway of apoptosis, the Bax/Bcl-2 mRNA ratio is the prominent characteristic. Therefore, the results of the Bax/Bcl-2 mRNA ratio in different groups are shown in Fig. 6B. The Bax/Bcl-2 mRNA ratio increased with increasing doses of X-ray radiation. The Bax/Bcl-2 mRNA ratios in the cells treated with 2, 4, and 6 Gy X-rays were equal to 1.36 ± 0.11 , 2.2 ± 0.07 , and 3.5 ± 0.28 , respectively. While these ratios in the NPs-treated cells followed by 2, 4, and 6 Gy X-ray significantly increased to 5.26 ± 0.7 , 10.87 ± 0.9 , and 23.3 ± 1.35 , respectively.

These results revealed that the apoptotic pathway and the expression of apoptotic-related genes may have a key role in the Fe₃O₄@Cus-PEG nanoparticles radiation dose enhancement effects.

Combined effect of nanoparticles and ionizing radiation To further investigate whether the Fe₃O₄@Cus-PEG nanoparticles combined with ionizing radiation had a synergistic effect on the cell viability measured by the MTT assay and the long-term viability determined by the clonogenic assay, the equations established by Ito et al. were used (Ito et al. 2007). As illustrated in Table 2, the MTT assay showed that the values of [NP + IR] and [NP] × [IR] were equal to 62% and 81.4% for 2 Gy X-ray, 41.1% and 65.2% for 4 Gy X-ray, and 25.1% and 42.9% for 6 Gy X-ray, respectively.

In addition, the survival fractions calculated for [NP + IR] were significantly lower than that of [NP] × [IR] at all doses of X-ray radiation ($P < 0.0001$). The results of the colony formation assay were consistent with the results of the MTT assay. These data revealed that the evaluated cytotoxicity effects of the combined treatment of Fe₃O₄@Cus-PEG nanoparticles and X-ray radiation were strongly synergistic.

Table 2 Analysis of the combined effect of Fe₃O₄@Cus-PEG nanoparticles and ionizing radiation. The values were represented by the mean ± SD of three independent experiments

Dose	Based on the MTT data			Based on the colony data		
	[NP + IR]	[NP] × [IR]/100	P value	[NP + IR]	[NP] × [IR]/100	P value
2 Gy	62 ± 1	81.4 ± 1.1	0.0001	56 ± 2.6	80.2 ± 5.3	0.0001
4 Gy	41.1 ± 1.3	65.2 ± 0.35	0.0001	31.6 ± 2.1	56 ± 0.47	0.0001
6 Gy	25.1 ± 1.4	42.9 ± 3.7	0.0001	15 ± 2	32.2 ± 4.7	0.0001

[NP], [IR], and [NP + IR] represent the percentage of cell viability or survival fraction after treatments with Fe₃O₄@Cus-PEG NPs, ionizing radiation, and combination of nanoparticles with ionizing radiation, respectively

Discussion

Radiotherapy is one of the most effective modalities for cancer therapy. The ionizing radiation dose is a critical limitation in radiotherapy treatment because of the damage to normal surrounding tissues. The physicochemical characteristic of nanoparticles makes them exceptional agents in different aspects of medicine to overcome some of the drawbacks (Her et al. 2017; Schaeue et al. 2015).

In this study, we synthesized biodegradable $\text{Fe}_3\text{O}_4@\text{Cus}$ -PEG nanoparticles as a radiosensitizer agent to improve the efficacy of ionizing radiation and reduce its side effects.

TEM images confirmed the semi-spherical shape of nanoparticles. Hydrodynamic diameter of nanoparticles was 31 nm. The small size of nanoparticles allows them to selectively enter cancer cells and accumulate there through the enhanced permeability and retention effect (Kulkarni et al. 2013).

The cytotoxicity analysis of $\text{Fe}_3\text{O}_4@\text{Cus}$ -PEG NPs using the MTT assay showed that nanoparticles induced dose-dependent toxicity. Magnetite nanoparticles at high doses can increase the generation of malonaldehyde and reactive oxygen species in cells. In addition, it leads to oxidative damage to DNA and apoptosis (Su et al. 2018; Watanabe et al. 2013). In addition, cell treatment with copper at high doses is associated with abnormalities and morphological changes that can cause cell death (Gupta et al. 2009).

So, cell treatment should be done with a concentration of nanoparticles that has low toxicity effects on cells. Therefore, the IC10 value of NPs was chosen for the treatment of HT-29 cells. The copper spinel ferrite superparamagnetic nanoparticles (CuFe_2O_4 SPM-NPs) were synthesized by Meidanchi et al. (2021). The cytotoxicity of nanoparticles was evaluated using the MTT assay. According to the results, the viability of MCF-7 cells after 4 h treatment with nanoparticles at the concentrations of 1, 10, and 100 $\mu\text{g}/\text{mL}$ was equal to 87.6, 85.5, and 64.4%, respectively. Whereas, in our study, the observed toxicity for $\text{Fe}_3\text{O}_4@\text{Cus}$ -PEG nanoparticles at the concentration of 5 mg/mL after 24 h treatment was 90%. This indicates that the cytotoxicity of the synthesized NPs in our study was remarkably lower than that of NPs synthesized by Meidanchi et al.

In this study, the efficacy of $\text{Fe}_3\text{O}_4@\text{Cus}$ -PEG NPs to improve the effects of ionizing radiation on cancer cells was evaluated using various analyses. As depicted in Fig. 3A, NPs-treated cells under X-ray exposure showed a significant reduction in cell viability as compared with the ionizing radiation-treated cells which indicate the radio-sensitizing effects of $\text{Fe}_3\text{O}_4@\text{Cus}$ -PEG NPs. Meidanchi et al. (2020) showed that $\text{Mg}(1-x)\text{Cu}x\text{Fe}_2\text{O}_4$ SPMNPs with $x = 0.6$ at the concentration of 1 $\mu\text{g}/\text{mL}$ and $x = 0.2$ at the concentration of 10 $\mu\text{g}/\text{mL}$ could act as a radiosensitizer agent and enhance the effects of 2 Gy ionizing radiation on MCF-7 cells.

The results of the MTT assay were evaluated by Compusyn software. The CI values and isobologram curve (Fig. 3B) obtained from the Compusyn software demonstrated that the combined treatments of $\text{Fe}_3\text{O}_4@\text{Cus}$ -PEG NPs and X-ray radiation (at all doses) had a synergetic effect on the HT-29 cancer cells. These results proved the advantages of our synthesized nanoparticles in combination with ionizing radiation. Huang et al. examined the radiosensitizing effects of heterogeneous copper selenide-gold nanoparticles (CSA) in the presence of megavoltage X-ray radiation (at different doses of 0, 2, 4, 6, and 8 Gy). Their results demonstrated that the interaction between CSA nanoparticles and radiotherapy + laser was synergistic and the data

points in the isobologram curve were under the line of additive effect (Huang et al. 2019). Whereas, we obtained the same results only with the copper sulfide superparamagnetic nanoparticles and ionizing radiation.

The cell survival curves and Fig. 4A showed that the proliferation of $\text{Fe}_3\text{O}_4@\text{Cus-PEG}$ NPs-treated HT-29 cells was significantly inhibited under X-ray exposure compared to the cells treated with the same doses of ionizing radiation ($P < 0.0001$) which represent the efficacy of the synthesized nanoparticles as a radiosensitizer agent. The SER obtained by D_{50} was 2.02 that indicating the toxicity of ionizing radiation enhances about 2 times in the presence of $\text{Fe}_3\text{O}_4@\text{Cus-PEG}$ NPs. The sensitivity enhancement ratio of copper selenide-gold nanoparticles calculated by Huang et al. was 1.6 (Q. Huang et al. 2019). Zhang et al. treated the U251 cells with the $\text{Fe}_3\text{O}_4@\text{Ag}$ nanoparticles and then exposed them to X-ray radiation at doses of 0, 2, 4, 6, and 8 Gy. In their study, the obtained SER value for $\text{Fe}_3\text{O}_4@\text{Ag}$ NPs was equal to 1.8 (Zhang et al. 2018). The sensitivity enhancement ratio of our nanoparticles was higher than that of these studies which indicates that the hybrid of copper sulfide and Fe_3O_4 NPs have the significant ability to improve the radiosensitivity of cancer cells.

Given that Table 1, the α parameter in the combined treatment (NP + IR) significantly increased in comparison with the single treatment (IR), while the β , SF_2 , D_{10} , D_{37} , and D_{50} parameters showed a reverse trend and decreased. These findings were in line with other studies (Yi et al. 2018; Zangeneh et al. 2019). As shown in Fig. 4B, the survival curve appeared linearly for the cells treated with nanoparticles and ionizing radiation. The presence of $\text{Fe}_3\text{O}_4@\text{Cus-PEG}$ NPs under X-ray radiation increases the amount of lethal damages and decreases the sub-lethal damages, which lead to the α and β parameters increase and decrease, respectively. Therefore, the shoulder region of the survival curve disappears and the curve becomes more linear (Hall et al. 2006).

As displayed in Table 2, the dominant synergistic effects were observed for the combined treatments of HT-29 colorectal cancer cells and the results were in complete agreement with the results of isobologram curves and combination index. $\text{Fe}_3\text{O}_4@\text{Cus-PEG}$ NPs were successfully used to enhance the effects of X-ray exposure on HT-29 cells.

The radiosensitizing effects of nanoparticles may be due to two factors: (1) the physical dose enhancement because of the increased production of high-energy secondary electrons through Compton interaction. The predominant interaction between 6 MV X-ray photons and copper sulfide or iron nanoparticles is Compton scattering (Alkhatib et al. 2009; McMahan et al. 2011) (2) the improvement of biological effects.

Iron oxide and copper nanoparticles can increase the intracellular ROS production by the Haber-Weiss and Fenton reaction (Huang et al. 2019; Klein et al. 2012). Jiang et al. revealed that the ROS production increased by the copper oxide nanoparticles (CuO NPs) under X-ray ionizing radiation (Jiang et al. 2019). Moreover, the radiosensitizing effect of copper sulfide and iron oxide NPs can be attributed to the increased apoptotic death (Liu et al. 2017; Zhang et al. 2018).

To understand the mechanisms involved in the radiosensitizing effects of $\text{Fe}_3\text{O}_4@\text{Cus-PEG}$ NPs, the concentration of intracellular nitric oxide and hydrogen peroxide, the activity of Glutathione Peroxidase as an antioxidant enzyme, and the mRNA expression levels of the apoptotic-related genes were assessed.

The Bax/Bcl-2 mRNA ratio has an outstanding role in the initiation of the intrinsic pathway of apoptosis when its ratio increases. Results illustrated that the addition of Fe₃O₄@Cus–PEG NPs to the HT-29 cells in the radiotherapy treatment at the doses of 2, 4, and 6 Gy increased the Bax/Bcl-2 ratio by 3.87, 4.9, and 6.6-fold, respectively (Fig. 6B). Our in vitro studies demonstrated that synthesized nanoparticles induced dose-dependent cell death in HT-29 colorectal cancer cells through apoptosis.

Our in vitro colorimetric assays demonstrated that the nitric oxide production and the intracellular hydrogen peroxide concentration significantly increased in the cells treated with the combination of radiation and nanoparticles (Fig. 5A, B). However, the GPX enzyme activity in the combined treatment groups significantly decreased compared to the radiation alone (Fig. 5C). The GPX enzyme activity in the NP-treated cells followed by 6 Gy X-ray radiation decreased by 2.2-fold in comparison with the 6 Gy ionizing radiation alone ($P < 0.0001$).

These results indicate that in the combined treatments, the oxidative stress increases that can lead to redox disequilibrium and increases the generation of ROS and nitric oxide. This can overcome the antioxidant defense capacity of the cells and ultimately increase the apoptotic death of cancer cells.

Conclusions

Fe₃O₄@Cus–PEG nanoparticles were synthesized and characterized. These nanoparticles enhanced the effects of 6 MV X-ray irradiation in a dose-dependent manner and increased the toxicity of ionizing radiation by about 2 times. Nanoparticles could enhance X-ray irradiation to destruct HT-29 cancer cells by increasing ROS generation, nitric oxide production, inducing apoptosis, and decreasing Glutathione peroxidase enzyme activity. Collectively, this study suggests that Fe₃O₄@Cus–PEG NPs can be used as a promising nano radio-sensitizing agent and the effects of X-ray radiation in the presence of nanoparticles were strongly synergistic.

Abbreviations

SER	Sensitizing enhancement ratio
NPs	Nanoparticles
CRC	Colorectal cancer
RT	Radiation therapy
EPR	Enhanced permeability and retention
ROS	Reactive oxygen species
Cu	Copper
SPIONs	Superparamagnetic iron oxide nanoparticles
MRI	Magnetic resonance imaging
IGRT	Image-guided radiotherapy
PVP	Poly Vinyl Pyrrolidone
PLGA	Poly Lactic Glycolic acid
PBCA	Poly butyl cyanoacrylate
PEG	Polyethylene glycol
DMSO	Dimethyl sulfoxide
FBS	Fetal Bovine Serum
MTT	3-(4,5-Dimethyl-thiazol-2-yl)-2,5-diphenyl-tetrazolium bromide
RPMI	Roswell Park Memorial Institute
TEM	Transmission electron microscope
DLS	Dynamic light scattering
XRD	X-ray diffraction
NO	Nitric oxide
GPX	Glutathione peroxidase
q-RT-PCR	Quantitative real-time polymerase chain reaction
DSB	Double-strand break

IR	Ionizing radiation
CI	Combination index
SD	Standard deviation
ANOVA	One-way analysis of variance

Acknowledgements

Not applicable.

Author contributions

SEM and MM performed laboratory in vitro examinations and all cytotoxic and genetic assays. SEM analyzed the data and was a major contributor in writing the manuscript. ASD synthesized nanoparticles and characterized them. All authors read and approved the final manuscript.

Funding

This work was supported by Urmia University of Medical Sciences (UMSU) under Grant No. 2830.

Availability of data and materials

The data sets used and/or analyzed during the current study are available from the corresponding author on reasonable request.

Declarations

Ethics approval and consent to participate

Not applicable.

Consent for publication

Not applicable.

Competing interests

The authors declare that they have no conflict of interest.

Received: 19 February 2022 Accepted: 11 August 2022

Published online: 19 August 2022

References

- Alkhatib A, Watanabe Y, Broadhurst JH (2009) The local enhancement of radiation dose from photons of MeV energies obtained by introducing materials of high atomic number into the treatment region. *Med Phys* 36(8):3543–3548
- Babaei M, Ganjalikhani M (2014) The potential effectiveness of nanoparticles as radio sensitizers for radiotherapy. *Biomol-pacts* 4(1):15
- Binjola A (2020) Interaction of radiation with matter practical radiation oncology. Springer, Cham, pp 3–11
- Brown KG, Solomon MJ, Mahon K, O'Shannassy S (2019) Management of colorectal cancer. *BMJ* 366:l4561
- Chen M-H, Hanagata N, Ikoma T, Huang J-Y, Li K-Y, Lin C-P, Lin F-H (2016) Hafnium-doped hydroxyapatite nanoparticles with ionizing radiation for lung cancer treatment. *Acta Biomater* 37:165–173
- Delorme R, Taupin F, Flaender M, Ravanat JL, Champion C, Agelou M, Elleaume H (2017) Comparison of gadolinium nanoparticles and molecular contrast agents for radiation therapy-enhancement. *Med Phys* 44(11):5949–5960
- Desouky O, Ding N, Zhou G (2015) Targeted and non-targeted effects of ionizing radiation. *J Radiat Res Appl Sci* 8(2):247–254
- Gao Y, Kang J, Lei Z, Li Y, Mei X, Wang G (2020) Use of the highly biocompatible Au nanocages@ PEG nanoparticles as a new contrast agent for in vivo computed tomography scan imaging. *Nanoscale Res Lett* 15(1):1–9
- Ghaferi M, Amari S, Vivek Mohrir B, Raza A, Ebrahimi Shahmabadi H, Alavi SE (2020) Preparation, characterization, and evaluation of cisplatin-loaded polybutylcyanoacrylate nanoparticles with improved in vitro and in vivo anticancer activities. *Pharmaceuticals* 13(3):44
- Goswami N, Luo Z, Yuan X, Leong DT, Xie J (2017) Engineering gold-based radiosensitizers for cancer radiotherapy. *Mater Horiz* 4(5):817–831
- Guo Z, Zhu S, Yong Y, Zhang X, Dong X, Du J, Xie J, Wang Q, Gu Z, Zhao Y (2017) Synthesis of BSA-coated BiOI@ Bi2S3 semiconductor heterojunction nanoparticles and their applications for radio/photodynamic/photothermal synergistic therapy of tumor. *Adv Mater* 29(44):1704136
- Gupta AK, Gupta M (2005) Synthesis and surface engineering of iron oxide nanoparticles for biomedical applications. *Biomaterials* 26(18):3995–4021
- Gupta A, Lutsenko S (2009) Human copper transporters: mechanism, role in human diseases and therapeutic potential. *Future Med Chem* 1(6):1125–1142
- Hadi F, Ghader A, Shakeri-Zadeh A, Asgari H, Farashahi A, Behruzi M, Ghaznavi H, Ardakani AA (2020) Magneto-plasmonic nanoparticle mediated thermo-radiotherapy significantly affects the nonlinear optical properties of treated cancer cells. *Photodiagn Photodyn Ther* 30:101785
- Hall EJ, Giaccia AJ (2006). *Radiobiology for the Radiologist* (Vol. 6): Philadelphia
- Hauser AK, Mitov MI, Daley EF, McGarry RC, Anderson KW, Hilt JZ (2016) Targeted iron oxide nanoparticles for the enhancement of radiation therapy. *Biomaterials* 105:127–135
- Her S, Jaffray DA, Allen C (2017) Gold nanoparticles for applications in cancer radiotherapy: mechanisms and recent advancements. *Adv Drug Deliv Rev* 109:84–101

- Huang Q, Zhang S, Zhang H, Han Y, Liu H, Ren F, Sun Q, Li Z, Gao M (2019) Boosting the radiosensitizing and photothermal performance of Cu₂-x Se nanocrystals for synergetic radiophotothermal therapy of orthotopic breast cancer. *ACS Nano* 13(2):1342–1353
- Huang C-L, Kumar G, Sharma GD, Chen F-C (2020) Plasmonic effects of copper nanoparticles in polymer photovoltaic devices for outdoor and indoor applications. *Appl Phys Lett* 116(25):253302
- Huynh M, Kempson I, Bezak E, Phillips W (2021) Predictive modeling of hypoxic head and neck cancers during fractionated radiotherapy with gold nanoparticle radiosensitization. *Med Phys* 48(6):3120–3133
- Ito A, Fujioka M, Yoshida T, Wakamatsu K, Ito S, Yamashita T, Jimbow K, Honda H (2007) 4-S-Cysteaminyphenol-loaded magnetite cationic liposomes for combination therapy of hyperthermia with chemotherapy against malignant melanoma. *Cancer Sci* 98(3):424–430
- Jiang X, Han Y, Zhang H, Liu H, Huang Q, Wang T, Sun Q, Li Z (2018) Cu–Fe–Se ternary nanosheet-based drug delivery carrier for multimodal imaging and combined chemo/photothermal therapy of cancer. *ACS Appl Mater Interfaces* 10(50):43396–43404
- Jiang Y-W, Gao G, Jia H-R, Zhang X, Zhao J, Ma N, Liu JB, Liu P, Wu F-G (2019) Copper oxide nanoparticles induce enhanced radiosensitizing effect via destructive autophagy. *ACS Biomater Sci Eng* 5(3):1569–1579
- Kiamohammadi L, Asadi L, Shirvalilou S, Khoei S, Khoei S, Soleymani M, Minaei SE (2021) Physical and biological properties of 5-fluorouracil polymer-coated magnetite nanographene oxide as a new thermosensitizer for alternative magnetic hyperthermia and a magnetic resonance imaging contrast agent: in vitro and in vivo study. *ACS Omega* 6(31):20192–20204
- Klein S, Sommer A, Distel LV, Neuhuber W, Kryschi C (2012) Superparamagnetic iron oxide nanoparticles as radiosensitizer via enhanced reactive oxygen species formation. *Biochem Biophys Res Commun* 425(2):393–397
- Kulkarni SA, Feng S-S (2013) Effects of particle size and surface modification on cellular uptake and biodistribution of polymeric nanoparticles for drug delivery. *Pharm Res* 30(10):2512–2522
- LaVerne JA (2000) OH radicals and oxidizing products in the gamma radiolysis of water. *Radiat Res* 153(2):196–200
- Liu Z, Xiong L, Ouyang G, Ma L, Sahi S, Wang K, Lin L, Huang H, Miao X, Chen W (2017) Investigation of copper cysteamine nanoparticles as a new type of radiosensitizers for colorectal carcinoma treatment. *Sci Rep* 7(1):1–11
- Maggiorella L, Barouch G, Devaux C, Pottier A, Deutsch E, Bourhis J, Borghi E, Levy L (2012) Nanoscale radiotherapy with hafnium oxide nanoparticles. *Future Oncol* 8(9):1167–1181
- Mao F, Wen L, Sun C, Zhang S, Wang G, Zeng J, Wang Y, Ma J, Gao M, Li Z (2016) Ultrasmall biocompatible Bi₂Se₃ nanodots for multimodal imaging-guided synergistic radiophotothermal therapy against cancer. *ACS Nano* 10(12):11145–11155
- McMahon SJ, Hyland WB, Muir MF, Coulter JA, Jain S, Butterworth KT, Schettino G, Dickson GR, Hounsell AR, O'Sullivan JM (2011) Biological consequences of nanoscale energy deposition near irradiated heavy atom nanoparticles. *Sci Rep* 1(1):1–10
- Meidanchi A (2020) Mg (1-x) Cu_xFe₂O₄ superparamagnetic nanoparticles as nano-radiosensitizer agents in radiotherapy of MCF-7 human breast cancer cells. *Nanotechnology* 31(32):325706
- Meidanchi A, Ansari H (2021) Copper spinel ferrite superparamagnetic nanoparticles as a novel radiotherapy enhancer effect in cancer treatment. *J Cluster Sci* 32(3):657–663
- Mi P, Dewi N, Yanagie H, Kokuryo D, Suzuki M, Sakurai Y, Li Y, Aoki I, Ono K, Takahashi H (2015) Hybrid calcium phosphate-polymeric micelles incorporating gadolinium chelates for imaging-guided gadolinium neutron capture tumor therapy. *ACS Nano* 9(6):5913–5921
- Minaei SE, Mozdarani H, Motazakker M, Mansouri M, Aghamiri SMR (2016) Evaluation of cytogenetic alterations in peripheral blood lymphocytes of esophageal cancer patients treated with radiotherapy or chemoradiotherapy using cytokinesis-blocked micronucleus assay. *Acta Med Iran* 54:9–14
- Nosrati H, Baghdadchi Y, Abbasi R, Barsbay M, Ghaffarlou M, Abhari F, Mohammadi A, Kavetsky T, Bochani S, Rezaeejam H, Rezaeejam H (2021) Iron oxide and gold bimetallic radiosensitizers for synchronous tumor chemoradiation therapy in 4T1 breast cancer murine model. *J Mater Chem B* 9(22):4510–4522
- Park J, Choi Y, Chang H, Um W, Ryu JH, Kwon IC (2019) Alliance with EPR effect: combined strategies to improve the EPR effect in the tumor microenvironment. *Theranostics* 9(26):8073
- Penninckx S, Heuskin A-C, Michiels C, Lucas S (2020) Gold nanoparticles as a potent radiosensitizer: a transdisciplinary approach from physics to patient. *Cancers* 12(8):2021
- Rae C, Tesson M, Babich JW, Boyd M, Sorensen A, Mairs RJ (2013) The role of copper in disulfiram-induced toxicity and radiosensitization of cancer cells. *J Nucl Med* 54(6):953–960
- Rosanoff A, Weaver CM, Rude RK (2012) Suboptimal magnesium status in the United States: are the health consequences underestimated? *Nutr Rev* 70(3):153–164
- Russell E, Dunne V, Russell B, Mohamud H, Ghita M, McMahon SJ, Butterworth KT, Schettino G, McGarry CK, Prise KM (2021) Impact of superparamagnetic iron oxide nanoparticles on in vitro and in vivo radiosensitisation of cancer cells. *Radiat Oncol* 16(1):1–16
- Rybka JD (2019) Radiosensitizing properties of magnetic hyperthermia mediated by superparamagnetic iron oxide nanoparticles (SPIONs) on human cutaneous melanoma cell lines. *Rep Pract Oncol Radiother* 24(2):152–157
- Schae D, McBride WH (2015) Opportunities and challenges of radiotherapy for treating cancer. *Nat Rev Clin Oncol* 12(9):527–540
- Schieber M, Chandel NS (2014) ROS function in redox signaling and oxidative stress. *Curr Biol* 24(10):R453–R462
- Shirvalilou S, Khoei S, Khoei S, Mahdavi SR, Raoufi NJ, Motevalian M, Karimi MY (2020) Enhancement radiation-induced apoptosis in C6 glioma tumor-bearing rats via pH-responsive magnetic graphene oxide nanocarrier. *J Photochem Photobiol, B* 205:111827
- Siegel RL, Miller KD, Jemal A (2019) Cancer statistics, 2019. *Cancer J Clin* 69(1):7–34
- Song L, Falzone N, Vallis KA (2016) EGF-coated gold nanoparticles provide an efficient nano-scale delivery system for the molecular radiotherapy of EGFR-positive cancer. *Int J Radiat Biol* 92(11):716–723

- Su H, Li Z, Lazar L, Alhamoud Y, Song X, Li J, Wang Y, Fiati kenston SS, Lqbal MZ, Wu, A. (2018) In vitro evaluation of the toxicity and underlying molecular mechanisms of Janus Fe₃O₄-TiO₂ nanoparticles in human liver cells. *Environ Toxicol* 33(10):1078–1088
- Sun L, Joh DY, Al-Zaki A, Stangl M, Murty S, Davis JJ, Baumann BC, Alonso-Basanta M, Kao GD, Tsourkas A (2016) Theranostic application of mixed gold and superparamagnetic iron oxide nanoparticle micelles in glioblastoma multiforme. *J Biomed Nanotechnol* 12(2):347–356
- Torres-Roca JF, Stevens CW (2008) Predicting response to clinical radiotherapy: past, present, and future directions. *Cancer Control* 15(2):151–156
- Wang Y, Wu Y, Liu Y, Shen J, Lv L, Li L, Yang L, Zeng J, Wang Y, Zhang LW (2016) BSA-mediated synthesis of bismuth sulfide nanotheranostic agents for tumor multimodal imaging and thermoradiotherapy. *Adv Func Mater* 26(29):5335–5344
- Wang Y, Tian D, Chu W, Li M, Lu X (2019) Nanoscaled magnetic CuFe₂O₄ as an activator of peroxymonosulfate for the degradation of antibiotics norfloxacin. *Sep Purif Technol* 212:536–544
- Watanabe M, Yoneda M, Morohashi A, Hori Y, Okamoto D, Sato A, Kurioka D, Nittami T, Hirokawa Y, Shiraishi T (2013) Effects of Fe₃O₄ magnetic nanoparticles on A549 cells. *Int J Mol Sci* 14(8):15546–15560
- Xie Y-H, Chen Y-X, Fang J-Y (2020) Comprehensive review of targeted therapy for colorectal cancer. *Signal Transduct Target Ther* 5(1):1–30
- Yi X, Chen L, Chen J, Maiti D, Chai Z, Liu Z, Yang K (2018) Biomimetic copper sulfide for chemo-radiotherapy: enhanced uptake and reduced efflux of nanoparticles for tumor cells under ionizing radiation. *Adv Func Mater* 28(9):1705161
- Zangeneh M, Nedaei HA, Mozdarani H, Mahmoudzadeh A, Salimi M (2019) Enhanced cytotoxic and genotoxic effects of gadolinium-doped ZnO nanoparticles on irradiated lung cancer cells at megavoltage radiation energies. *Mater Sci Eng, C* 103:109739
- Zhang B, Shan Y, Chen K (2017) A facile approach to fabricate of photothermal functional Fe₃O₄@ CuS microspheres. *Mater Chem Phys* 193:82–88
- Zhang X, Liu Z, Lou Z, Chen F, Chang S, Miao Y, Zhou Z, Hu X, Feng J, Ding Q (2018) Radiosensitivity enhancement of Fe₃O₄@ Ag nanoparticles on human glioblastoma cells. *Artificial Cells, Nanomedicine, and Biotechnology* 46(sup1):975–984

Publisher's Note

Springer Nature remains neutral with regard to jurisdictional claims in published maps and institutional affiliations.

Ready to submit your research? Choose BMC and benefit from:

- fast, convenient online submission
- thorough peer review by experienced researchers in your field
- rapid publication on acceptance
- support for research data, including large and complex data types
- gold Open Access which fosters wider collaboration and increased citations
- maximum visibility for your research: over 100M website views per year

At BMC, research is always in progress.

Learn more biomedcentral.com/submissions

